Six Degree of Freedom Computation of the F-15E Entering a Spin

James R. Forsythe*
Cobalt Solutions, LLC, Springfield OH, 45504
USAF Reserves, Air Force Office of Scientific Research
William Z. Strang†
Cobalt Solutions, LLC, Springfield OH, 45504
Kyle D. Squires‡
MAE Department, Arizona State University, Tempe, AZ 85287

A six-degree-of-freedom computational model is used to calculate the the motion of an F-15E entering a spin. The massively separated flowfield around the aircraft is predicted using Detached-Eddy Simulation (DES). These simulations build on previous calculations of the aircraft at high angle of attack, both at static conditions and with a prescribed rotary motion. Predictions are assessed via comparison to Boeing's stability and control database. A small bump is added to the nose of the aircraft that triggers an asymmetric vortex shedding on the forebody, as observed in flight and wind tunnel tests at high angles of attack. The yawing moment produced by the asymmetric vortices drives the spin. Three attempted spin entries are calculated. The first attempt releases the aircraft from rest and in a horizontal attitude. The aircraft drops, the nose rapidly tucks down, and the aircraft recovers. The aircraft passes through the high angle of attack regime too quickly to develop a significant spin rate due to the asymmetric vortex shedding around the forebody. The remaining two attempts prescribe a rotary motion around the center of gravity and the freestream velocity vector with the aircraft at 90° angle of attack and descending vertically at Mach 0.3. The two attempts differ only in the initial direction of rotation. For one case, the asymmetric vortex shedding results in an anti-spin yawing moment. In this case the aircraft rotation rate rapidly decreases, the nose tucks down, and the aircraft recovers. For the second attempt, an oscillatory spin is entered and maintained for over five revolutions. The mean angle of attack, descent rate, and spin rate match well the expected conditions from the stability and control database. However, bank oscillations grow over time, and eventually reduce the effective angle of attack sufficiently to eliminate the asymmetric vortex shedding on the nose, reducing the spin rate. The aircraft then begins a recovery. The calculations were performed on 512 to 1024 processors allowing a rapid turn around despite the very large number of timesteps required.

*Director of Research, Senior Member AIAA
†Director of Development
‡Professor, Member of AIAA

I. Introduction

NUMERICAL simulation of the flow around complex configurations offers a powerful tool for analysis, e.g., a means to screen configurations prior to costly, hazardous and time-consuming flight tests. One example is spin testing in which Computational Fluid Dynamics (CFD) could be used to provide detailed information on stability, spin modes, etc. Though spins have been a maneuver that is safely taught in many aviation schools, "the stall-spin is one of the major causes of light airplane accidents even today."[1] A similar problem is the possible "tumble" of flying-wing aircraft, which could become a "show-stopper" in commercial applications (unless perhaps absolute stall protection could be considered established through electronic limiters). None of today's tools for such problems are based on a direct CFD solution of the flow.

Although flight testing is perhaps the optimum approach to determining an aircraft's spin characteristics, it cannot be used as a design tool since it requires a completed aircraft to test. Wind tunnel testing is often performed on working design models, but there are many inadequacies inherent to the process, including issues of dynamic scaling and Reynolds number effects.[2] There are also several analytical methods that have been used to predict spinning tendencies of aircraft. However, "the airplane spin is not very amenable for theoretical analysis because of nonlinear, inertial cross coupling between the longitudinal and lateral degrees of freedom. Furthermore, the aerodynamics of the spinning airplane are extremely complex because of extensive flow separation over the wing and tail surfaces."[1]

Computational Fluid Dynamics represents a relatively newer arena for spin research and engineering. It is less costly than other forms of testing and can be employed in earlier phases of the design process. CFD also allows for a more detailed examination of the flowfield than either wind tunnel, flight, or analytical methods. However, spins represent the type of flow that historically has been very challenging for CFD to accurately predict. This is primarily the result of large regions of separated, three-dimensional and unsteady turbulent flow around the aircraft. These aspects defeat most models, which is especially debilitating for spin prediction since the separated flow regions mediate the interference between separate control surfaces, notably the horizontal and vertical tails, which are known to have great control over spin.

Most current engineering approaches, even to the prediction of unsteady flows, are based on solution of the Reynolds-averaged Navier-Stokes (RANS) equations. The turbulence models employed in RANS methods, at first sight, parameterize the entire spectrum of turbulent motions; in practice some flow conditions "push" RANS solutions into unsteady behavior, typically with alternating vortex shedding. While often adequate in steady flows with no regions of flow reversal, or possibly exhibiting shallow separations, it appears inevitable that RANS turbulence models will be unable to accurately predict the phenomena dominating flows characterized by massive separations. Unsteady massively separated flows are characterized by geometry-dependent and three-dimensional turbulent eddies. These eddies, arguably, are what defeats RANS turbulence models, of any complexity.

To overcome the deficiencies of RANS models for predicting massively separated flows, Spalart *et al.*[3] proposed Detached-Eddy Simulation (DES) with the objective of developing a numerically feasible and accurate approach combining the most favorable elements of RANS models and Large Eddy Simulation (LES). The primary advantage of DES is that it can be applied at high Reynolds numbers (as can Reynolds-averaged techniques) but also, grid permitting, resolves geometry-dependent, unsteady three-dimensional turbulent motions as in LES. Typically, LES behavior takes place outside the boundary layers.

DES has been applied by the authors to prediction of the flow around the static (non-moving)[4] configuration at high angle of attack and prescribed rotary motions[5] of the F-15E. Since the motions were prescribed, inertial effects were not considered. The present investigation extends these earlier works by computing the motion of the F-15E entering a spin, which requires incorporation of the inertia of the airplane into the computational model as well as the capacity to compute the motion with six degrees of freedom.

Important to determining the spin characteristics of the F-15E (and many jet fighter aircraft) are forebody aerodynamics. At high angles of attack the rounded forebody of the F-15E produces asymmetric vortices which produce a large yawing moment.[6] Although this effect would not be expected for a symmetric body, it can be caused by extremely small disturbances near the tip of the forebody (such as paint chips

or manufacturing imperfections), and consequently it is always effectively present, even without sideslip. Because of the low aspect ratio of the F-15E and the strong yawing moment from the forebody, the aircraft spin is closer to flat, with yaw being the primary mode of motion.

The current effort focuses on the F-15E because of the availability of an extensive stability and control database.[7] This database was compiled from an extensive series of flight tests, including spins. Gaps in the flight test were filled with wind tunnel testing. The primary goal of the current work is to use flight test data to assess the entire computational strategy for predicting the spin of an F-15E. DES forms the basis of the turbulence treatment, a six-degree of freedom model is coupled to rigid body grid motion in order to model the spin. The aircraft is released from either prescribed motions or from rest. Three cases are calculated, with one case resulting in an oscillatory spin that lasts five rotations before bank oscillations drop the effective angle of attack, and allow the aircraft to recover.

For calculations of complex configurations at high Reynolds numbers, high-performance computation is essential. In this work, solutions of the compressible Navier-Stokes equations on unstructured grids are obtained using the commercial code *Cobalt*.[8] The numerical method is based on a finite-volume approach and is second-order accurate in space and time. The method is point-implicit and permits CFL numbers as large as 10^6 for steady-state computations.[9] Turbulence-resolving simulations are necessarily time dependent, and for DES the code is run in a time-accurate fashion. The computations are performed in parallel using the Message Passing Interface.[10] Between 512 and 1024 processors are used as part of a DoD Capabilities Application Project.

II. Computational Approach

A. Spalart-Allmaras Model

The Spalart-Allmaras (referred to as 'S-A' throughout) one-equation model[11] solves a single partial differential equation for a variable $\widetilde{\nu}$ which is related to the turbulent viscosity. The differential equation is derived by "using empiricism and arguments of dimensional analysis, Galilean invariance and selected dependence on the molecular viscosity."[11] The model includes a wall destruction term that reduces the turbulent viscosity in the log layer and laminar sublayer and trip terms that provides a smooth transition from laminar to turbulent flow. In the present computations, the trip term was not active, and the equation was

$$\frac{D\widetilde{\nu}}{Dt} = c_{b1}\widetilde{S}\,\widetilde{\nu} - c_{w1}f_w\left[\frac{\widetilde{\nu}}{d}\right]^2 + \frac{1}{\sigma}\left[\nabla\cdot\left((\nu+\widetilde{\nu})\,\nabla\widetilde{\nu}\right) + c_{b2}\left(\nabla\widetilde{\nu}\right)^2\right]$$

The turbulent viscosity is determined via,

$$\nu_t = \widetilde{\nu}\, f_{v1}, \qquad f_{v1} = \frac{\chi^3}{\chi^3 + c_{v1}^3}, \qquad \chi \equiv \frac{\widetilde{\nu}}{\nu}, \tag{1}$$

where ν is the molecular viscosity. Using S to denote the magnitude of the vorticity, the modified vorticity $\widetilde{S}$ is defined as,

$$\widetilde{S} \equiv S + \frac{\widetilde{\nu}}{\kappa^2 d^2} f_{v2}\,, \qquad f_{v2} = 1 - \frac{\chi}{1+\chi f_{v1}}\,, \tag{2}$$

where d is the distance to the closest wall. The wall destruction function, f_w is,

$$f_w = g\left[\frac{1+c_{w3}^6}{g^6+c_{w3}^6}\right]^{\frac{1}{6}}, \qquad g = r + c_{w2}(r^6 - r)\,, \qquad r \equiv \frac{\widetilde{\nu}}{\widetilde{S}\kappa^2 d^2}\,. \tag{3}$$

The closure coefficients are given by:

$$\begin{array}{ccc} c_{b1} = 0.1355 & \sigma = 2/3 & c_{b2} = 0.622 \\ \kappa = 0.41 & c_{w1} = \frac{c_{b1}}{\kappa^2} + \frac{(1+c_{b2})}{\sigma} & c_{w2} = 0.3 \\ c_{w3} = 2 & c_{v1} = 7.1 & \end{array} \tag{4}$$

B. Detached-Eddy Simulation

The DES formulation in this study is based on a modification to the Spalart-Allmaras RANS model[11] such that the model reduces to its RANS formulation near solid surfaces and to a subgrid model away from the wall.[12] The basis is to attempt to take advantage of the usually adequate performance of RANS models in the thin shear layers where these models are calibrated and the power of LES for resolution of geometry-dependent and three-dimensional eddies. The DES formulation is obtained by replacing in the S-A model the distance to the nearest wall, d, by $\widetilde{d}$, where $\widetilde{d}$ is defined as,

$$\widetilde{d} \equiv \min(d, C_{DES}\Delta)\,. \tag{5}$$

In Eqn. (5) for the current study, Δ is the largest distance between the cell center under consideration and the cell center of the neighbors (i.e., those cells sharing a face with the cell in question). In "natural" applications of DES, the wall-parallel grid spacings (e.g., streamwise and spanwise) are at least on the order of the boundary layer thickness and the S-A RANS model is retained throughout the boundary layer, i.e., $\widetilde{d} = d$. Consequently, prediction of boundary layer separation is determined in the 'RANS mode' of DES. Away from solid boundaries, the closure is a one-equation model for the SGS eddy viscosity. When the production and destruction terms of the model are balanced, the length scale $\widetilde{d} = C_{DES}\Delta$ in the LES region yields a Smagorinsky scaling for the eddy viscosity $\widetilde{\nu} \propto S\Delta^2$. Analogous to classical LES, the role of Δ is to allow the energy cascade down to the grid size; roughly, it makes the pseudo-Kolmogorov length scale, based on the eddy viscosity, proportional to the grid spacing. The additional model constant $C_{DES} = 0.65$ was set in homogeneous turbulence[13] and is used without modification in this study.

C. Code Details

Computations are performed using the commercial unstructured flow solver *Cobalt*. Strang *et al.*[8] validated the numerical method on a number of problems, including the Spalart-Allmaras model (which forms the core of the DES model). Tomaro *et al.*[9] converted the code from explicit to implicit, enabling CFL numbers as high as 10^6. Grismer *et al.*[10] parallelized the code, yielding a linear speedup on as many as 1024 processors. The Parallel METIS (ParMetis) domain decomposition library of Karypis *et al.*[14] is also incorporated into *Cobalt*. ParMetis divides the grid into nearly equally sized zones that are then distributed among the processors.

The numerical method is a cell-centered finite-volume approach applicable to arbitrary cell topologies (e.g, hexahedrals, prisms, tetrahdra). The spatial operator uses the exact Riemann Solver of Gottlieb and Groth,[15] least squares gradient calculations using QR factorization to provide second-order accuracy in space, and TVD flux limiters to limit extrema at cell faces. A point implicit method using analytic first-order inviscid and viscous Jacobians is used for advancement of the discretized system. For time-accurate computations, a Newton sub-iteration scheme is employed, and the method is second-order accurate in time.

D. Grid motion

Simulation of rigid-body motion is achieved through an Arbitrary Lagrangian Eulerian (ALE) formulation, where the grid is neither stationary nor follows the fluid motion. The conservation equations are solved in an inertial reference frame, but the spatial operator is modified so that the advection terms are relative to the (non-inertial) grid reference frame. This requires simple modifications to many boundary conditions and to the initial conditions for the Riemann problem. The inviscid and viscous work terms due to the grid velocity must also be removed from the spatial operator. The ALE formulation also forces certain modifications to the time-centered implicit temporal operator. A number of Newton sub-iterations are used to reduce errors associated with integrating over the timestep with an implicit temporal operator. The method has been applied to a pitching prolate spheroid[16] and a spinning forebody[17] with good agreement to experiments. For the six-degree of freedom model, a two stage Runge-Kutta loop is wrapped around the flow solver loop in order to integrate the six-degree of freedom equations.

III. Results

A. Approach

A stable spin was provided from the stability and control database[7] for a clean aircraft with a symmetric fuel load. The condition detailed the spin rate and the force and moment coefficients static and spinning. The spin was predicted from the database by an in-house code that predicted a spin state by balancing the force and moment coefficients with inertial forces and engine inertial effects. Moments of inertia in the current calculations were matched to the provided moments of inertia for the symmetric fuel load at an altitude of 30,000 feet. These conditions resulted in a predicted spin of 100 degrees per second at 65° angle-of-attack, a small sideslip, and a descent rate of Mach 0.3.

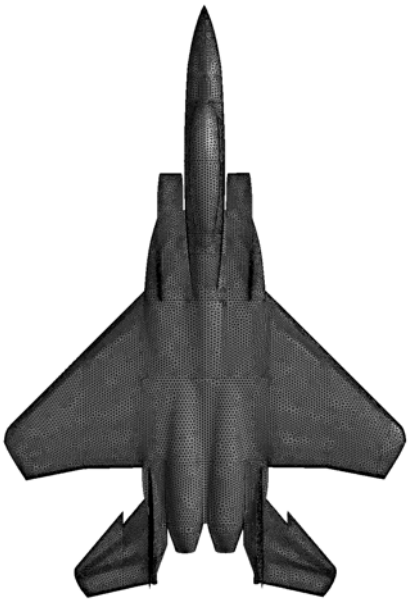

Figure 1. Top view of the surface mesh on the F-15E.

B. Calculation Details

Forsythe *et al.*[4] performed a grid resolution study using VGRIDns[18] on a half-aircraft model of the F-15E at $\alpha = 65°$ and $\beta = 0°$ in preparation for the current work. Three grids were used (2.85×10^6, 5.9×10^6, and 10.0×10^6 cells) with a $\sqrt{2}$ difference in spacing near the body in each coordinate direction between successive grids. The fine grid DES predictions agreed with the database to within 5% of the lift, drag, and pitching moment – the expected uncertainty of the database. By examining pressure slices along the forebody, wing, and tail, it was determined that the coarse grid was sufficient to provide grid-independent pressures on the wing. The forebody and the tail, however, required the finest grid resolution. The grid spacing for the current effort was guided by these results. The coarse grid spacing was retained (roughly) on the wing, while the grid density was increased on the tail and forebody. The resulting full aircraft grid (both sides were modeled) resulted in a grid containing 6.5×10^6 cells – see Figures 1 and 2. The distance from solid surfaces to the first cell center normal to the wall was constant, resulting in an average distance in wall units of 0.7. Cell growth in the wall-normal direction was specified using a geometric stretching factor of 1.25.

As previously discussed, the F-15E has a non-zero yaw moment at $\alpha = 65°$ and $\beta = 0°$ due to asymmetric vortex shedding on the forebody due to small imperfections. This effect is crucial to predicting the spin since the induced yawing moment is a large factor in driving the motion. Wurtzler[6] reproduced this effect computationally on an isolated F-15 forebody by adding a small bump on one side of the forebody above the midline and close to the front, the same approach is adopted in this work. Since the bump was only on one side of the aircraft, the full aircraft was gridded, rather than mirroring a half-aircraft model as possible on configurations with a symmetry plane. Surface pressures and streamlines are shown for an S-A RANS calculation in Figure 3. Despite the fact that the calculation was performed at zero sideslip, the vortices rapidly became asymmetric, causing a large difference in pressures on opposite sides of the forebody. This in turn causes a significant yawing moment due to the long moment arm of the forebody.

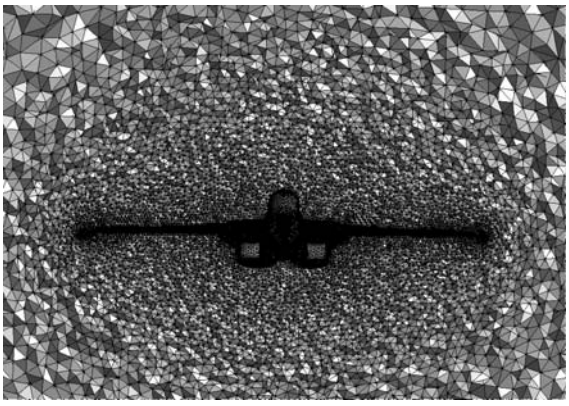

Figure 2. Cutting plane showing the grid near the middle of the F-15E wing.

The bump is also visible on the blown up view in Figure 3 (on the right side, as the pilot sits). The pressures predicted are in qualitative agreement with previous computations and experiments[6] shown in Figure 4 that were performed at a slightly lower angle of attack and for a laminar flow.

Static RANS and DES predictions reported in Forsythe *et al.*[5] as well as calculation of a prescribed spin motion have been obtained using the current grid. These results were important for providing a baseline assessment of mesh resolution and building confidence in use of that grid for six-DOF calculations.

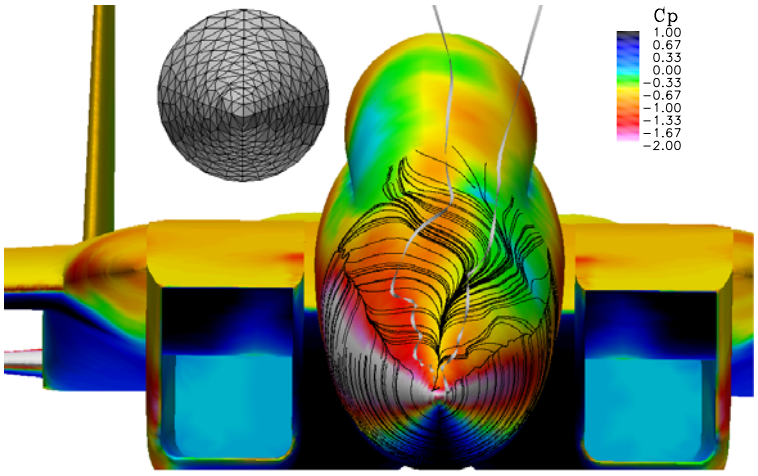

Figure 3. View of the asymmetric vortex shedding on the F-15E at $\alpha = 65°$ and no sideslip, SA RANS. Surface colored by pressure, surface streamlines in black, streamlines along vortex cores in grey. Zoomed view of the mesh on the forebody showing the bump on the right side (as the pilot sits).

C. Benchmarks

This work was performed as part of a Department of Defense Capabilities Application Project (CAP), sponsored by the DoD High Performance Computing Modernization Office. The purpose of a CAP is to demonstrate the capability of large parallel systems (2000-4000 processors) when dedicated to a single project. Code scalability is key to using these large machines effectively, so prior to production run, benchmarks were performed on several machines, with the results show in Figure 5.

The number of timesteps per minute is relatively low due to the use of five Newton subiterations per timestep, and the use of the two stage Runge-Kutta. This increases the cost per step by six times compared to a steady state calculation, but is necessary to accurately handle grid motion and the DOF integration. All three machines show good scalabilty with super-linear speed-up to a greater or lesser extent. The super-linear speed-up is caused by increased cache efficiency as the fixed problem size is broken down into smaller elements as the number of processors increases. This occurs in other unstructured codes as well.

Using 1000 processors, around 11 timesteps per minute are obtained, which will subsequently give a revolution every 8 hours of run time for the timestep selected (see below), indicating that many revolutions can be obtained in less than a week.

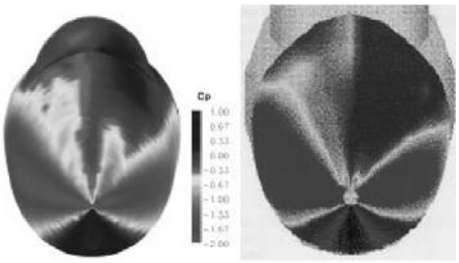

Figure 4. Computed (left) and measured (right) pressure coefficients of the laminar flow over an isolated F-15 forebody at $\alpha = 62°$.[6]

D. Six-DOF

Three attempted spin entries were calculated at conditions matching an altitude of 30,000 ft standard day. The timestep based on previous work was specified as $\Delta t = 0.013c/U_\infty$, leading to approximately 5000 timesteps per revolution.

The first attempt released the aircraft from rest and in a horizontal attitude. The aircraft dropped, the nose rapidly tucked down, and the aircraft recovered. The aircraft passed through the high angle of attack regime too quickly to develop a significant spin rate due to the asymmetric vortex shedding (although the simulations did show that the nose of the aircraft moved right a few degrees).

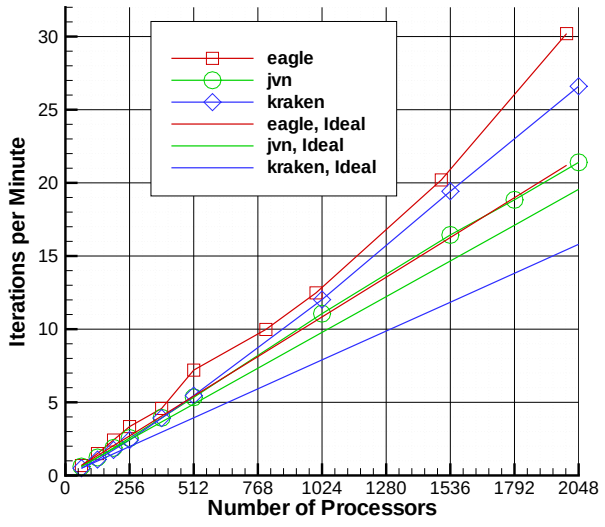

Figure 5. Actual vs. ideal iterations per minute vs. number of processors on several new DoD HPC systems.$6.5x10^6$ cell grid, five Netwon subiterations, two-stage Runge-Kutta.

The second two attempts prescribed a rotary motion around the center of gravity and the freestream velocity vector with the aircraft at 90° angle of attack and descending vertically at Mach 0.3. This is similar to spin tunnel tests in which the model is dropped into the tunnel with some spin. The two attempts differed only in the initial direction of rotation. After the flow had adjusted from an initial transient, the aircraft was released into six degrees of freedom. The first case started the spin in the left direction, with the resulting orientation plotted versus time in Figure 6. The spin angle (θ) is defined as the angle between an arbitrary vector in the horizontal plane, and the longitudinal axis of the aircraft projected onto the horizontal plane. The yawing moment from the asymmetric vortices on the nose were anti-spin for this case. Thus, the spin rate rapidly decreased, which allowed the nose to drop out of the high angle of attack range, and the aircraft recovered within two turns.

For the final case, the initial spin was in the appropriate direction, with the resulting orientation angles plotted versus time in Figure 7. For this case the asymmetric vortex shedding on the nose caused a pro-spin yawing moment, and the spin rate was sustained very close to 100°/sec for five revolutions. The angle of attack oscillated around 65° as predicted by the stability and control database. However, bank (side-slip) oscillations grew over time, which eventually lowered the effective angle of attack low enough so that the vortex shedding was no longer asymmetric, and the yaw rate decreased. Near the end of the run, the spin rate has been greatly reduced, and it seems that the aircraft will recover given time. It should be noted that the control surfaces for the current runs are neutral (not pro-spin) which makes the stabilized spin difficult to achieve. Spin tunnel tests achieved a stable spin about three out of ten tosses into the tunnel[a]. The descent rate during the initial five turns remains within a percent of Mach 0.3, indicating that the drag is a good match to the stability and control database.

These calculations required over 40,000 timesteps, leading to the large CPU requirement. The runs used 512 to 1024 processors, with 40,000 timesteps requiring less than four days of run time. Although costly, this shows that by using large parallel machines, and a scalable code, spin testing could be accomplished with an acceptable turn around time currently, or in the near future.

IV. Summary

Detached-Eddy Simulation was used to predict the massively separated flow around the F-15E with a six degree-of-freedom model. Three separate initial conditions were used in an attempt to enter the spin. Spinning the aircraft in the pro-spin direction (according to the asymmetry of the forebody vortices) was required in order to enter the spin. An oscillatory spin was demonstrated for five turns, however oscillations in roll eventually took the aircraft out of the spin. This may be caused by starting far enough off of the stable spin conditions.

[a] *Personal communication*, Charles M. Fremaux, NASA Langley

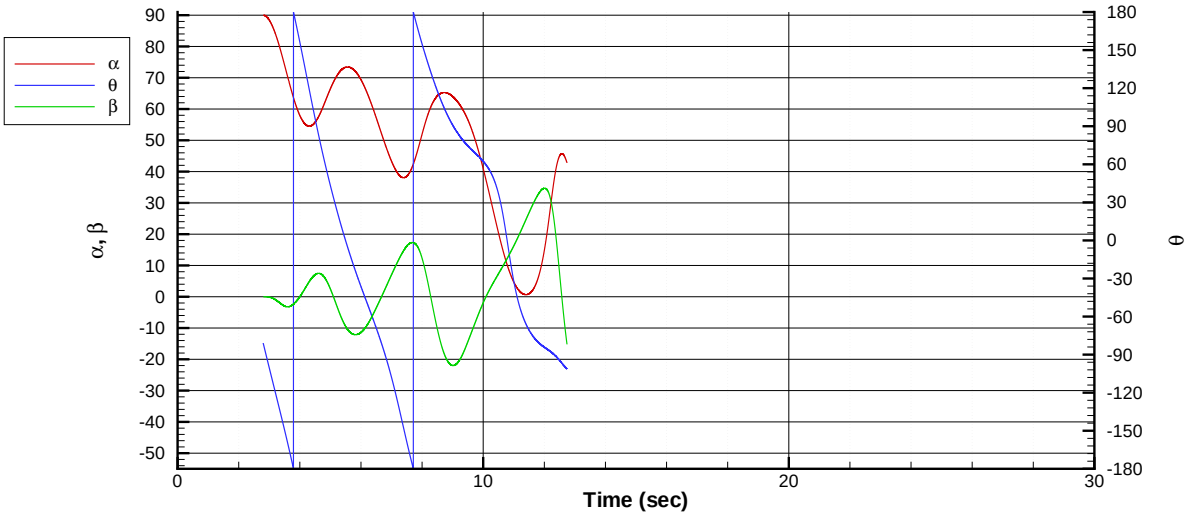

Figure 6. Angle of attack (α), Spin angle (θ), and side-slip angle (β) vs. time for the left spinning case.

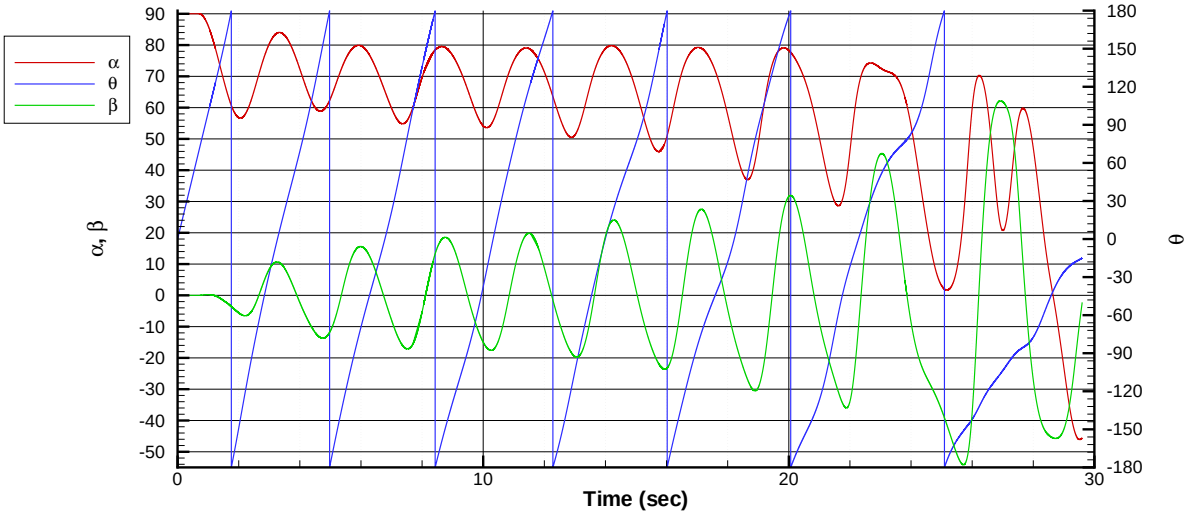

Figure 7. Angle of attack (α), Spin angle (θ), and side-slip angle (β) vs. time for the right spinning case.

V. Acknowledgments

The authors gratefully acknowledge the support of AFOSR Grant F49620-00-1-0050 (Program Manager: Dr. Tom Beutner). The authors are also grateful for the assistance of Dr. Glen Peters, Dr. Ken Walck, and Dr. Walt Labozzetta of Boeing Military, who provided the stability and control database and the F-15E geometry. Many helpful discussions of DES and aircraft spin with Dr. Philippe Spalart of Boeing Commercial Airplanes are gratefully acknowledged. Also, there were many informative discussions with Mike Fremaux of NASA Langley on the F-15 spin tunnel tests. Benchmarks for the CAP were performed at the ARL, NAVO, and ASC Major Shared Resource Centers. Finally, the project would not have been possible without the support and cpu hours at the ARL MSRC provided by a Capabilities Application Project.

References

[1]Pamadi, B.N., Performance, Stability, Dynamics, and Control of Airplanes, AIAA Education Series, pp. 627–672, 1998.

[2]Pauley,H., Ralston, J., and Dickes, E., "Experimental Study of the Effects of Reynolds number on High Angle of Attack Aerodynamic Characteristics of Forebodies during rotary motion," *NASA CR 195033*, Jan. 1995.

[3]Spalart, P.R., Jou, W.H., Strelets, M. and Allmaras, S.R., 1997, "Comments on the Feasibility of LES for Wings, and on a Hybrid RANS/LES Approach,", *First AFOSR International Conference on DNS/LES*, Ruston, Louisiana, USA.

[4]Forsythe, J.R., Squires, K.D., Wurtzler, K.E., Spalart, P.R., "Detached-Eddy Simulation of the F-15E at High Alpha," *AIAA Journal of Aircraft*, Vol. 41, No. 2, 2004, pp. 193-200.

[5]Forsythe, J.R., Wentzel, J.F., Squires, K.D., Wurtzler, K.E., Spalart, P.R., "Computation of Prescribed Spin for a Rectangular Wing and for the F-15E Using Detached-Eddy Simulation," *AIAA 2003-0839*, Jan. 2003.

[6]Wurtzler, K.E., "An Effectiveness Study of F-15 Forebody Flow Analysis Using $Cobalt_{60}$," *AIAA 99-0536*, 1999.

[7]Peters, G. and Walck, K., "Excerpts from the F-15E Stability and Control Database", *Personal Communication*, Dec. 2000.

[8]Strang, W.Z., Tomaro, R.F, Grismer, M.J., 1999, "The Defining Methods of $Cobalt_{60}$: a Parallel, Implicit, Unstructured Euler/Navier-Stokes Flow Solver," *AIAA 99-0786*, January 1999.

[9]Tomaro, R.F., Strang, W.Z., and Sankar, L.N., 1997, "An Implicit Algorithm for Solving Time Dependent Flows on Unstructured Grids," *AIAA 97-0333*, January 1997.

[10]Grismer, M. J., Strang, W. Z., Tomaro, R. F. and Witzemman, F. C., "Cobalt: A Parallel, Implicit, Unstructured Euler/Navier-Stokes Solver," *Advances in Engineering Software*, Vol. 29, No. 3-6, pp. 365—373, 1998.

[11]Spalart, P.R. and Allmaras, S.R., 1994, "A One-Equation Turbulence Model for Aerodynamic Flows," *La Recherche Aerospatiale* **1**, pp. 5-21.

[12]Spalart, P.R. (2000), "Strategies for Turbulence Modeling and Simulations", *International Journal of Heat and Fluid Flow*, **21**, p. 252-263.

[13]Shur, M., Spalart, P. R., Strelets, M., and Travin, A, 1999, "Detached-Eddy Simulation of an Airfoil at High Angle of Attack", 4th Int. Symp. Eng. Turb. Modelling and Measurements, Corsica, May 24-26, 1999.

[14]Karypis, G., Schloegel, K. and Kumar, V., 1997, "ParMETIS: Parallel Graph Partitioning and Sparse Matrix Ordering Library Version 1.0", University of Minnesota, Department of Computer Science, Minneapolis, MN 55455, July 1997.

[15]Gottlieb, J.J. and Groth, C.P.T., 1988, "Assessment of Riemann Solvers for Unsteady One-Dimensional Inviscid Flows of Perfect Gases", *Journal of Computational Physics*, **78**, pp. 437-458.

[16]Kotapati-Apparao, R., Forsythe, J., Squires, K., "Computation of the Flow Over a Maneuvering Spheroid," *AIAA 2003-0269*, Jan 2003.

[17]Viswanathan, A., Klismith, K., Forsythe, J., Squires, K., "Detached-Eddy Simulation Around a Rotating Forebody," *AIAA 2003-0263*, Jan 2003.

[18]Pirzadeh, S., 1996, "Three-dimensional Unstructured Viscous Grids by the Advancing Layers Method," *AIAA Journal*, **34**, pp. 43-49.